LETTER

doi:10.1038/nature09557

Tumour vascularization via endothelial differentiation of glioblastoma stem-like cells

Lucia Ricci-Vitiani[1]*, Roberto Pallini[2]*, Mauro Biffoni[1], Matilde Todaro[3], Gloria Invernici[4], Tonia Cenci[5], Giulio Maira[2], Eugenio Agostino Parati[4], Giorgio Stassi[3,6], Luigi Maria Larocca[5] & Ruggero De Maria[1,7]

Glioblastoma is a highly angiogenetic malignancy, the neoformed vessels of which are thought to arise by sprouting of pre-existing brain capillaries. The recent demonstration that a population of glioblastoma stem-like cells (GSCs) maintains glioblastomas[1,2] indicates that the progeny of these cells may not be confined to the neural lineage[3]. Normal neural stem cells are able to differentiate into functional endothelial cells[4]. The connection between neural stem cells and the endothelial compartment seems to be critical in glioblastoma, where cancer stem cells closely interact with the vascular niche and promote angiogenesis through the release of vascular endothelial growth factor (VEGF) and stromal-derived factor 1 (refs 5–9). Here we show that a variable number (range 20–90%, mean 60.7%) of endothelial cells in glioblastoma carry the same genomic alteration as tumour cells, indicating that a significant portion of the vascular endothelium has a neoplastic origin. The vascular endothelium contained a subset of tumorigenic cells that produced highly vascularized anaplastic tumours with areas of vasculogenic mimicry in immunocompromised mice. *In vitro* culture of GSCs in endothelial conditions generated progeny with phenotypic and functional features of endothelial cells. Likewise, orthotopic or subcutaneous injection of GSCs in immunocompromised mice produced tumour xenografts, the vessels of which were primarily composed of human endothelial cells. Selective targeting of endothelial cells generated by GSCs in mouse xenografts resulted in tumour reduction and degeneration, indicating the functional relevance of the GSC-derived endothelial vessels. These findings describe a new mechanism for tumour vasculogenesis and may explain the presence of cancer-derived endothelial-like cells in several malignancies.

From archival material, we selected a group of glioblastomas showing both remarkable angiogenesis and nuclear accumulation of mutant p53 in tumour cells (Supplementary Table 1). In 83.3% (20/24) of these tumours, we found cells with nuclear accumulation of mutant p53 that lined the lumens of capillaries and/or vascular glomeruli (Supplementary Fig. 1a and Supplementary Table 1). Double immunohistochemistry analysis of p53 and CD31 demostrated the endothelial phenotype of the p53-positive cells facing the lumen of the vessels (Supplementary Fig. 1b). Mouse and human tumour-associated endothelial cells can harbour chromosomal alterations[10–12]. To assess whether a subset of endothelial cells showed glioblastoma-specific chromosomal aberrations, we analysed the tumour vasculature in 15 glioblastomas by combined CD31 immunofluorescence and fluorescence *in situ* hybridization (FISH) using probes for the centromere of chromosome 10 (Cep10), for the telomere of chromosome 19 (Tel19q), and a locus-specific probe on chromosome 22 (breakpoint cluster region locus q11.2; LSI22). In all the tumours carrying aneuploidy for one or more of these chromosomes, we detected a substantial fraction of endothelial cells bearing the same chromosomal aberrations (Supplementary Fig. 1c). Interestingly, double immunostaining of vascular glomeruli in glioblastoma revealed a significant number of $GFAP^+$ microvascular cells showing an aberrant endothelial/glial phenotype (Supplementary Fig. 1d). Thus, a variable number of endothelial cells in glioblastoma seem to originate from the tumour. To quantify the contribution of tumour-derived endothelial cells to glioblastoma vasculature, we used FISH to analyse purified $CD31^+/CD144^+$ (VE-Cadherin$^+$) endothelial cells from freshly dissociated glioblastoma specimens (Fig. 1a). Again, we detected $CD31^+/CD144^+$ endothelial cells that shared the same chromosomal alterations as the tumour cells in any given glioblastoma harbouring aberrations of chromosomes 10, 19 and 22 (Fig. 1b and Supplementary Table 2). The amount of endothelial cells with tumour-specific chromosomal changes ranged between 20 and 90% of the sorted cells (mean 60.7 ± 28.1 standard deviations (s.d.)).

We assessed further the phenotype of sorted $CD31^+/CD144^+$ glioblastoma cells by immunofluorescence, which showed that the vast majority of these cells (83.9 ± 4.2%; range 79–90%) expressed the mature endothelial cell marker von Willebrand factor (vWF), although a substantial proportion of them (30.9 ± 21.3%; range 10–76%) co-expressed vWF and GFAP (Fig. 1c, d). Thus, it seems that the $CD31^+/CD144^+$ cells harbouring chromosomal aberrations are glioblastoma-derived endothelial cells that either differentiated towards the canonical endothelial lineage ($GFAP^-$) or showed a mixed endothelial/glial phenotype ($GFAP^+$), whereas the euploid fraction is likely to represent endothelial cells derived from normal brain vessels. *In vitro* experiments using a microvascular culture of fresh $CD31^+$ cells isolated by magnetic microbeads from glioblastoma samples confirmed the existence of endothelial cells with aberrant GFAP expression (Supplementary Fig. 2a–c), as well as the presence of a substantial number of aneuploid endothelial cells (Supplementary Fig. 2d, e). Grafting of freshly purified $CD31^+/CD144^+$ cells showed that three of five glioblastomas contained tumorigenic endothelial cells that produced highly vascularized anaplastic tumours (Supplementary Fig. 3a–c). These cells, however, lost their tumorigenic activity on *in vitro* culture with endothelial medium (Supplementary Fig. 3a).

Although there is no general agreement on the definiton and markers identifying so-called cancer stem cells, there is good evidence that GSCs can be enriched by the use of anti-CD133 antibodies or through the generation of clusters of undifferentiated cells (neurospheres) in serum-free media containing epidermal growth factor (EGF) and basic fibroblast growth factor (FGF)[1,5,7,13,14]. We demonstrated recently that GSCs can differentiate into mesenchymal cells, giving rise to osteoblastic and chondrocytic cells[3]. To determine the potential contribution to the angiogenic process of GSCs, we cultivated glioblastoma neurospheres and primary glioblastoma differentiated cells under endothelial conditions, or $CD133^+/CD31^-$ and $CD133^-/CD31^-$ cells derived from the

[1]Department of Hematology, Oncology and Molecular Medicine, Istituto Superiore di Sanità, Viale Regina Elena 299, Rome 00161, Italy. [2]Department of Neurosurgery, Catholic University of Rome, Largo Francesco Vito 1, Rome 00168, Italy. [3]Department of Surgical and Oncological Sciences, University of Palermo, Via Liborio Giuffrè 5, Palermo 90127, Italy. [4]U. O. Cerebrovascular Disease Cellular Neurobiology Laboratory, Fondazione IRCCS, Neurological Institute "Carlo Besta", Via Celoria 11, 20133 Milan, Italy. [5]Institute of Pathology, Catholic University of Rome, Largo Francesco Vito 1, Rome 00168, Italy. [6]Cellular and Molecular Oncology, Istituto di Ricovero e Cura a Carattere Scientifico Fondazione Salvatore Maugeri, Via S. Maugeri 6, Pavia 27100, Italy. [7]Mediterranean Institute of Oncology, Via Penninazzo 7, 95029, Viagrande, Catania, Italy.
*These two authors contributed equally to the manuscript.

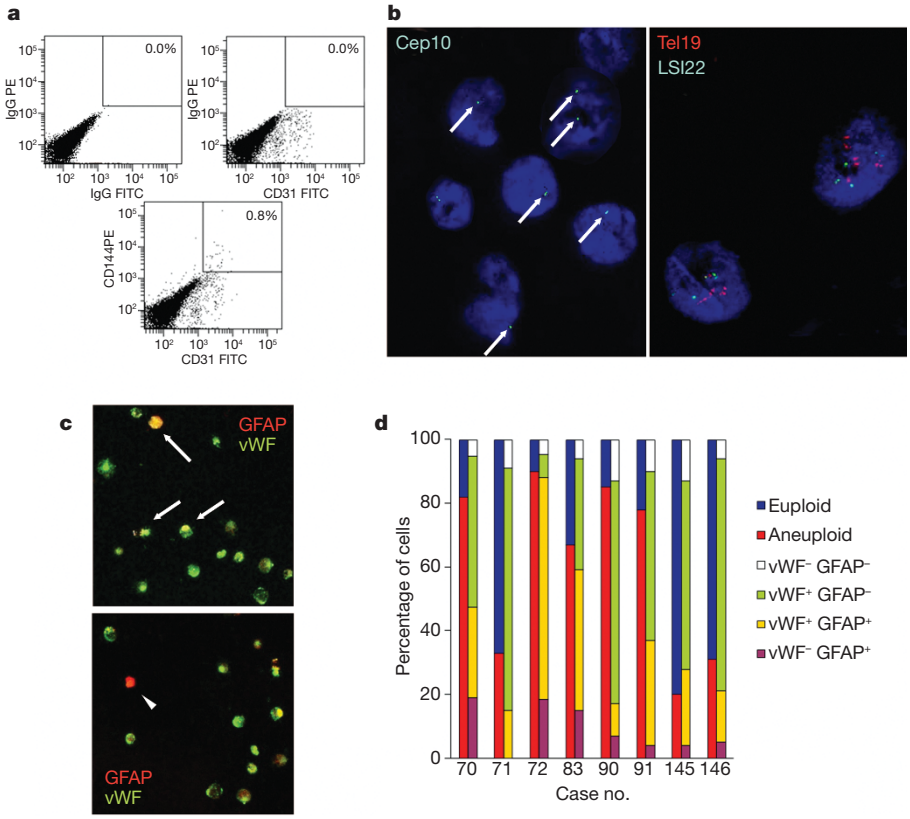

Figure 1 | Microvascular endothelial cells isolated from glioblastoma harbour tumour-specific chromosomal aberrations. **a**, $CD31^+/CD144^+$ cells were isolated from surgical glioblastoma specimens ($n = 15$). FITC, fluorescein isothiocyanate; PE, phycoerythrin. **b**, Sorted cells were analysed by interphase FISH assay for tumour-specific chromosomal changes, such as monosomy of Cep10 (left, arrows) or polisomy of Tel19 and LSI22 (right). **c**, The phenotype of the $CD31^+/CD144^+$ sorted cells was further analysed by anti-GFAP and anti-vWF immunofluorescence. A fraction of the $CD31^+/CD144^+$ cells coexpressed GFAP and vWF (arrows), indicating an aberrant endothelial/glial phenotype. A minority of sorted cells were $GFAP^+/vWF^-$. **d**, Quantification of results from FISH and immunofluorescence analysis.

same tumours. Whereas cells enriched in GSCs generated microvascular cultures of $CD31^+$ and $Tie2^+$ cells, neither differentiated cells nor the U87MG cell line were able to produce endothelial-like cells (Fig. 2a). Such GSC-derived endothelial cells showed considerable tube-forming ability, together with low-density lipoprotein (LDL) uptake and endothelial nitric oxide synthase (eNOS) expression, which were completely absent in differentiated tumour cells and in the U87MG cell line (Fig. 2b–d and Supplementary Fig. 4). Unsupervised gene-expression analysis of glioblastoma and endothelial cells showed that neural-differentiated glioblastoma cells and normal endothelial cells constitute the two more distant groups in a dendrogram in which tumour endothelial cells cluster between normal endothelial cells and glioblastoma neurospheres (Supplementary Fig. 5).

To investigate the ability of GSCs to form endothelial vessels *in vivo*, we measured the relative amount of murine versus human endothelial cells within glioblastoma neurosphere xenografts (Fig. 3a). Flow cytometry analysis with human- and mouse-specific antibodies showed that about 70% of the $CD31^+$ cells from the inner portion of the tumour were of human origin, whereas nearly all the $CD31^+$ cells in the tumour capsule were murine (Fig. 3b). Likewise, human $CD144^+$ cells were detected only in the core and not in the tumour capsule (Fig. 3b). Immunohistochemistry of subcutaneous and intracranial xenografts showed that glioblastoma neurosphere-derived tumours contained human vessels labelled by human-specific anti-CD31, whereas xenografts generated with U87MG or other glioma cell lines grown in serum did not (Fig. 3c, Supplementary Fig. 6a and data not shown). The presence of human-derived endothelial cells was confirmed by labelling sections of tumour xenografts obtained with GFP^+ glioblastoma neurospheres with anti-GFP and anti-human CD31 antibodies (Supplementary Fig. 6b). Moreover, immunofluorescence staining with validated human-specific endothelial antibodies showed that these cells expressed consistently CD34, CD144 and VEGFR2 (Fig. 3d) but not the stem-cell markers SSEA-1 and CD133 (Supplementary Fig. 6c). Such human-specific endothelial antigens identified microvascular structures containing circulating erythrocytes (Fig. 3d and Supplementary Fig. 6a), indicating the functional relevance of human angiogenesis in the tumour xenografts. Of note, a similar formation of human endothelial cells was observed in subcutaneous xenografts obtained with the injection of freshly purified $CD133^+/CD31^-$ cells, whereas $CD133^-/CD31^-$ cell xenografts contained only mouse endothelial vessels (Supplementary Fig. 7).

To trace *in vivo* angiogenesis, we injected RFP-labelled glioblastoma neurospheres into transgenic NOD/SCID mice expressing GFP under the Tie2 promoter. Examination of a thick-section plane by confocal microscopy showed that GFP^+ mouse vessels were primarily outside the tumours (Supplementary Fig. 8a). To exclude the occurrence of fusion between tumour and mouse endothelial cells, we stained tumour xenograft sections with anti-human/mouse Tie2 and CD31 antibodies. Although CD31 staining showed the presence of vessels containing both mouse and human $CD31^+$ cells at the periphery of the tumour, the majority of endothelial cells inside the tumour mass did not express mouse Tie2 and were of human origin in the absence of fusion (Supplementary Fig. 8b, c). Moreover, FISH analysis of nuclei extracted from microdissected vascular structures of GSC xenografts confirmed the absence of murine chromosomes in human cells (Supplementary Fig. 9). Together, these findings demonstrate that the tumour xenografts obtained by injection of human glioblastoma neurospheres develop an intrinsic vascular network composed by

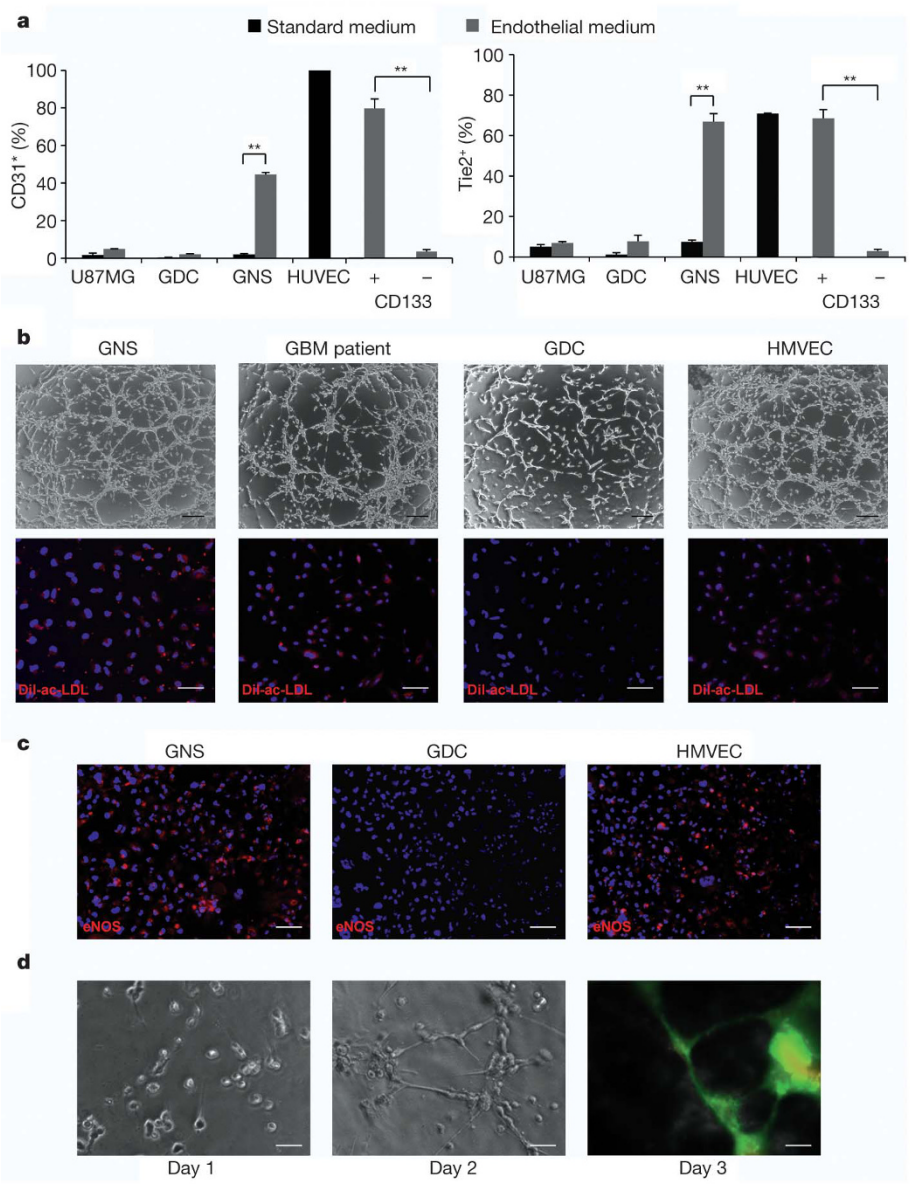

Figure 2 | GSCs cultured under endothelial differentiation conditions develop morphological, phenotypical and functional features of endothelial cells. **a**, Flow cytometry analysis of human umbilical vein endothelial cells (HUVEC), glioblastoma neurospheres (GNS), primary glioblastoma cells cultured in serum (GDC), U87MG, $CD31^-/CD133^+$ and $CD31^-/CD133^-$ cells from freshly dissociated glioblastomas. Cells were cultured under standard (black) or endothelial (grey) condition. Error bars represent the mean ± s.d. ($n = 4$). $^{**}P < 0.001$. **b**, Tube formation (top) and LDL-uptake (bottom) assay on cells under endothelial conditions as above (GNS and GDC), endothelial cells isolated from glioblastoma patients (GBM patients) and human dermal microvascular endothelial cells (HMVEC). DiI-ac-LDL, 1,1′-dioetadeeyl-3,3,3′,3′-tetramethylindocarboeyanine-perchlorate-acetylated LDL. Scale bars, 200 μm (top) and 50 μm (bottom). **c**, Immunofluorescence for eNOS in HMVEC, GNS and GDCs treated as above. Scale bar, 100 μm. **d**, *In vitro* perfusion assay on three-dimensional glioblastoma neurosphere-derived endothelial culture injected with fluorescein. Scale bar, 50 μm. One representative of four independent experiments performed in blind is shown for **b**, **c** and **d**.

tumour cells with an aberrant endothelial phenotype. To determine whether the GSC-derived endothelial cells contribute to tumour growth, we transduced glioblastoma neurospheres with a lentiviral vector containing the herpes simplex virus thymidine kinase gene (*tk*) under the control of the transcription-regulatory elements of Tie2 (Tie2-*tk*; Supplementary Fig. 10a), so that the tumour-derived endothelial cells would be sensitive to ganciclovir[15,16]. For this experiment, we selected glioblastoma neurospheres with no detectable expression of Tie2 (Supplementary Fig. 11). Control cells included glioblastoma neurospheres tranduced with an empty viral vector and U87MG cells transduced either with Tie2-*tk* or with a vector conferring constitutive expression of Tk (PGK-*tk*, Supplementary Fig. 10a). One week after ganciclovir administration, TdT-mediated dUTP nick end labelling (TUNEL) and double immunofluorescence labelling with anti-Tie2 antibodies in tumour subcutaneous xenografts showed selective apoptosis of the endothelial compartment only in animals injected with Tie2-*tk* neurospheres, whereas PGK-*tk* tumours contained a considerable number of apoptotic nuclei both in tumour and endothelial cells (Fig. 4a). Moreover, tumours generated by Tie2-*tk* neurospheres underwent a significant size reduction four weeks after ganciclovir administration, whereas control GSC xenografts increased their size over the same time interval (Fig. 4b).

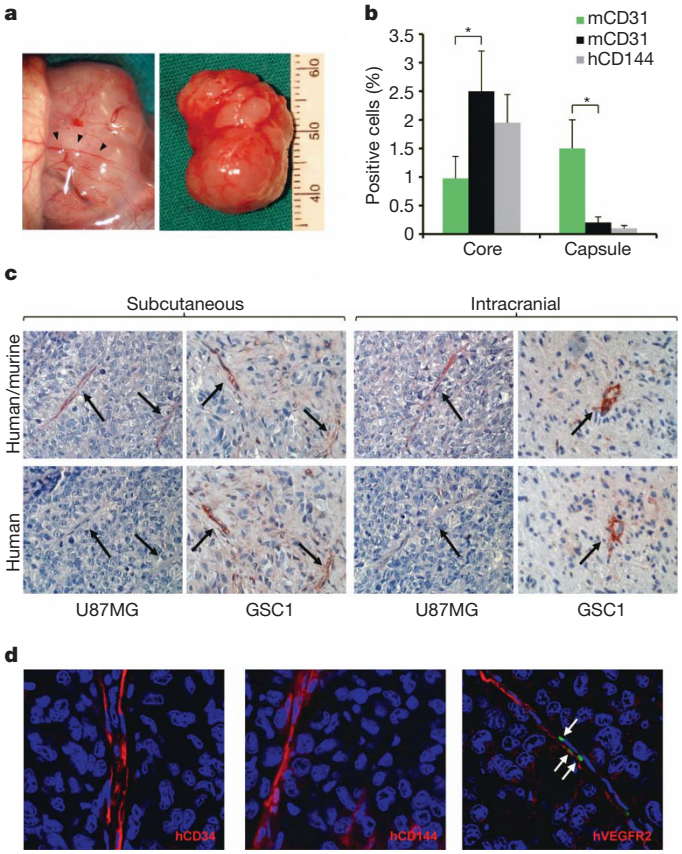

Figure 3 | Human origin of endothelial cells in glioblastoma neurosphere xenografts. **a**, Explanted subcutaneous xenograft obtained by injection of glioblastoma neurospheres. Detail of murine vessels on the surface of the xenograft (left, black arrowheads) and tumour after capsule removal (right). **b**, FACS evaluation of murine $CD31^+/CD45^-$ (mCD31), human CD31 (hCD31) and human CD144 (hCD144) in the capsule and core of the tumour (mean ± s.d., $n = 4$, $^*P < 0.05$). **c**, Immunohistochemistry of glioblastoma neurosphere (GSC1) and U87MG xenografts using either an anti-human CD31 or anti-human and murine CD31 (one out of four different glioblastoma neurosphere samples and serum-grown cell lines are shown). **d**, Immunofluorescence of tumour xenograft sections labelled with anti-human CD34 (left), anti-human CD144 (middle) or anti-human VEGFR2 (right). Arrows indicate circulating erythrocytes. Data represent one of four independent experiments obtained with different glioblastoma neurosphere samples.

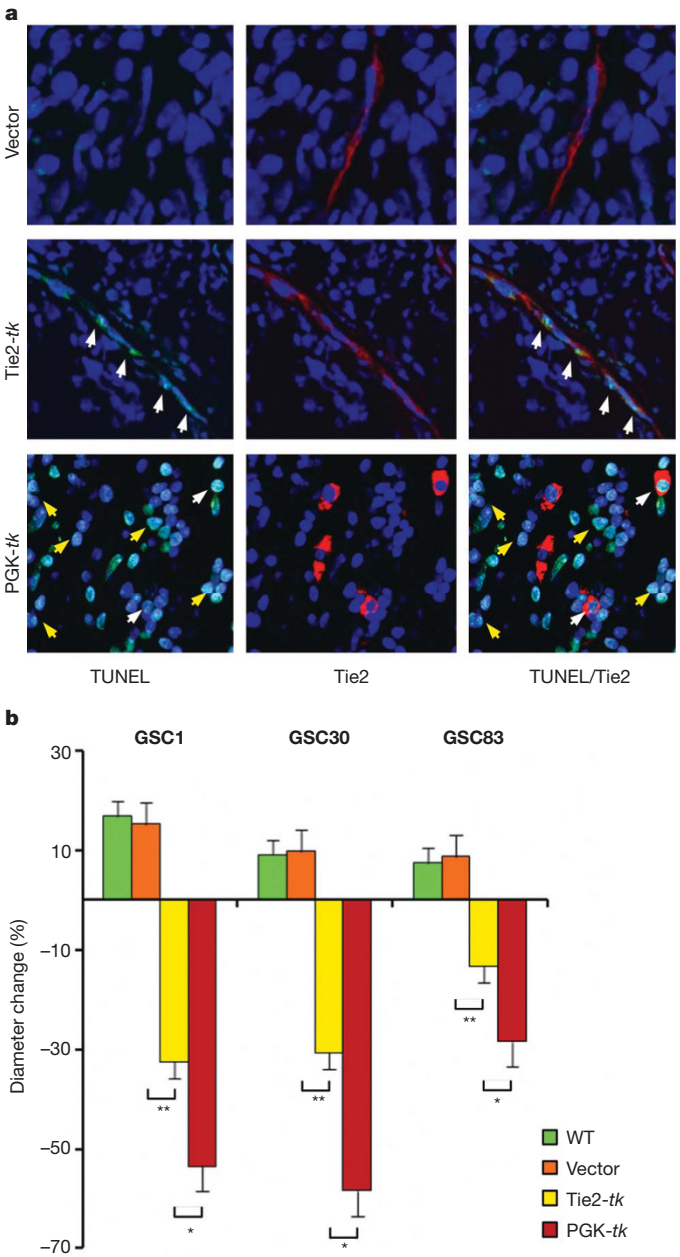

Figure 4 | Selective targeting of glioblastoma neurosphere-derived endothelial cells impairs the growth of subcutaneous tumour xenografts. **a**, Double immunofluorescence using anti-TUNEL and anti-Tie2 in xenografts from Tie2-*tk*, PGK-*tk* and vector glioblastoma neurosphere cells one week after ganciclovir administration. Arrows indicate apoptotic $Tie2^+$ (white) and $Tie2^-$ (yellow) cells. **b**, Tumour size measured four weeks after ganciclovir administration in xenograft obtained from three different glioblastoma neurosphere samples either untransduced (wild type (WT)) or transduced with vector, Tie2-*tk* or PGK-*tk*. Error bars are mean ± s.d. of three different experiments. $^*P < 0.005$, $^{**}P < 0.001$.

Histological examination revealed massive degeneration in the tumour xenografts developed by injection of Tie2-*tk* neurospheres. Four weeks after ganciclovir treatment, these tumours were completely devoid of vascular glomeruli, tiny capillaries with ongoing phenomena of endothelial disruption being the only residual vascular structures (Supplementary Fig. 10b). Although all PGK-*tk* tumours degenerated massively, U87MG Tie2-*tk* xenografts were not affected by ganciclovir treatment (Supplementary Fig. 10c, d), confirming that this cell line was unable to generate endothelial cells. These findings indicate that GSC-derived angiogenesis is essential for tumour survival. Moreover, mouse models based on adherent cell lines grown in serum do not seem suitable for the study of glioblastoma angiogenesis.

Here we demonstrated that GSCs are able to differentiate in functional endothelial cells. Such angiogenic potential could be inherited from normal neural stem cells, which have been shown to differentiate in endothelial cells both *in vitro* and *in vivo*[4]. The formation of fluid-conducting networks by nonendothelial cells has been described for melanomas, sarcomas, breast, ovary, lung and prostate carcinomas[17,18] as a result of vasculogenic mimicry, which is a feature associated with a pluripotent gene expression pattern in aggressive tumour cells[19].

The ability of cancer stem-like cells to directly contribute to the tumour vasculature by endothelial cell differentiation represents a new mechanism of angiogenesis that might not be restricted to glioblastoma. A similar endothelial potential may be shared by $CD44^+$ cells purified from ovarian cancer[20]. However, the existence of tumour-derived endothelial cells in ovarian cancer has not been demonstrated yet. Endothelial-like cells with cancer-specific genomic alterations have been described in other tumour types, such as lymphoma and neuroblastoma[11,12]. Although the angiogenic activity of cancer stem-like cells has not been investigated in other tumours, it is likely that the

endothelial cells bearing tumour-specific alterations derive from cancer cells endowed with stem-cell plasticity. Likewise, the vasculogenic mimicry might represent an incomplete differentiation of cancer stem-like cells towards the endothelial lineage, as indicated by the aberrant mixed phenotype of glioblastoma xenografts generated by the subset of $CD31^+/CD144^+$ cells that retain tumorigenic activity.

Our findings may have considerable therapeutic implications. On the one hand, endothelial cells bearing the same genomic alteration as cancer cells may show a different sensitivity to conventional anti-angiogenic treatments, such as VEGF/VEGFR targeting. On the other hand, our data indicate the possibility of targeting the process of GSC differentiation into endothelial cells, thus offering new therapeutic options for cancer treatment.

METHODS SUMMARY

Cell culture. Glioblastoma neurosphere cultures were established from freshly dissociated surgical specimens as described[3,21,22]. Primary cultures of glioblastoma differentiated cells were obtained by plating cells from freshly dissociated samples in DMEM-F12 medium containing 10% FBS. For primary culture of glioblastoma microvascular endothelial cells, $CD31^+$ cells were purified using Miltenyi Microbead Kit (Miltenyi Biotech) according to manufacturer's instructions and grown in endothelial basal medium (EBM Bullet kit; Biowhittaker Cambrex).

Immunohistochemistry, immunofluorescence and flow cytometry. Immunohistochemistry was performed as described[22] on deparaffinized sections of glioblastoma tissue. For immunofluorescence, cells were fixed with 4% paraformaldehyde and permeabilized in 0.1% Triton X-100. Cytofluorimetric analysis was performed using a FACS Canto flow cytometer (Becton Dickinson). Cell sorting was performed with a FACS Aria cell sorter (Becton Dickinson).

Interphase FISH and combined immunohistochemistry and FISH (FICTION). Single- and dual-probe interphase FISH was performed as described[3]. Images were captured using a high-resolution black and white CCD microscope camera AxioCam MRm REV 2 (Karl Zeiss) and analysed using AxioVision 4 multichannel fluorescence basic workstation (Karl Zeiss).

Lentiviral infection. Selective targeting of the cells expressing endothelial phenotype was obtained by modifying the pRRLsin.Tie2p.TKiresGFP.spre lentiviral vector provided by L. Naldini[15,16]. Viral particle production and GSC infection were performed as previously described[23].

***In vivo* experiments.** Nude athymic and SCID mice (female, 4–5 weeks of age; Charles River) were used. Partially dissociated glioblastoma neurospheres were used for both orthotopic and subcutaneous injection, typically 10^5 and 5×10^5, respectively. For *in vivo* endothelial targeting, mice were injected with Tie2-*tk* glioblastoma neurospheres into the right flank and control vector glioblastoma neurospheres into the left flank. After having developed bilateral nodules mice received ganciclovir at 50 mg kg^{-1} day^{-1} intraperitoneally for 5 days. Ganciclovir-treated mice were killed at different time points to collect samples for histology and immunofluorescence.

Statistical analysis. Student's *t*-test was used to analyse data using Statistica (version 5.5; Statsoft) or Fig.P (version 2.7; Biosoft) softwares.

Full Methods and any associated references are available in the online version of the paper at www.nature.com/nature.

Received 22 October 2009; accepted 13 September 2010.
Published online 21 November 2010.

1. Singh, S. K. *et al.* Identification of human brain tumour initiating cells. *Nature* **432,** 396–401 (2004).
2. Vescovi, A. L., Galli, R. & Reynolds, B. A. Brain tumour stem cells. *Nature Rev. Cancer* **6,** 425–436 (2006).
3. Ricci-Vitiani, L. *et al.* Mesenchymal differentiation of glioblastoma stem cells. *Cell Death Differ.* **15,** 1491–1498 (2008).
4. Wurmser, A. E. *et al.* Cell fusion-independent differentiation of neural stem cells to the endothelial lineage. *Nature* **430,** 350–356 (2004).
5. Bao, S. *et al.* Stem cell-like glioma cells promote tumor angiogenesis through vascular endothelial growth factor. *Cancer Res.* **66,** 7843–7848 (2006).
6. Folkins, C. *et al.* Glioma tumor stem-like cells promote tumor angiogenesis and vasculogenesis via vascular endothelial growth factor and stromal-derived factor 1. *Cancer Res.* **69,** 7243–7251 (2009).
7. Calabrese, C. *et al.* A perivascular niche for brain tumor stem cells. *Cancer Cell* **11,** 69–82 (2007).
8. Gilbertson, R. J. & Rich, J. N. Making a tumour's bed: glioblastoma stem cells and the vascular niche. *Nature Rev. Cancer* **7,** 733–736 (2007).
9. Lathia, J. D. *et al.* Integrin α6 regulates glioblastoma stem cells. *Cell Stem Cell* **6,** 421–432 (2010).
10. Hida, K. *et al.* Tumor-associated endothelial cells with cytogenetic abnormalities. *Cancer Res.* **64,** 8249–8255 (2004).
11. Streubel, B. *et al.* Lymphoma-specific genetic aberrations in microvascular endothelial cells in B-cell lymphomas. *N. Engl. J. Med.* **351,** 250–259 (2004).
12. Pezzolo, A. *et al.* Tumor origin of endothelial cells in human neuroblastoma. *J. Clin. Oncol.* **25,** 376–383 (2007).
13. Singh, S. K. *et al.* Identification of a cancer stem cell in human brain tumors. *Cancer Res.* **63,** 5821–5828 (2003).
14. Galli, R. *et al.* Isolation and characterization of tumorigenic, stem-like neural precursors from human glioblastoma. *Cancer Res.* **64,** 7011–7021 (2004).
15. De Palma, M., Venneri, M. A. & Naldini, L. *In vivo* targeting of tumor endothelial cells by systemic delivery of lentiviral vectors. *Hum. Gene Ther.* **14,** 1193–1206 (2003).
16. De Palma, M., Venneri, M. A., Roca, C. & Naldini, L. Targeting exogenous genes to tumor angiogenesis by transplantation of genetically modified hematopoietic stem cells. *Nature Med.* **9,** 789–795 (2003).
17. Hendrix, M. J., Seftor, E. A., Hess, A. R. & Seftor, R. E. Vasculogenic mimicry and tumour-cell plasticity: lessons from melanoma. *Nature Rev. Cancer* **3,** 411–421 (2003).
18. Dome, B., Hendrix, M. J., Paku, S., Tovari, J. & Timar, J. Alternative vascularization mechanisms in cancer: pathology and therapeutic implications. *Am. J. Pathol.* **170,** 1–15 (2007).
19. Maniotis, A. J. *et al.* Vascular channel formation by human melanoma cells *in vivo* and *in vitro*: vasculogenic mimicry. *Am. J. Pathol.* **155,** 739–752 (1999).
20. Alvero, A. B. *et al.* Molecular phenotyping of human ovarian cancer stem cells unravels the mechanisms for repair and chemoresistance. *Cell Cycle* **8,** 158–166 (2009).
21. Eramo, A. *et al.* Chemotherapy resistance of glioblastoma stem cells. *Cell Death Differ.* **13,** 1238–1241 (2006).
22. Pallini, R. *et al.* Cancer stem cell analysis and clinical outcome in patients with glioblastoma multiforme. *Clin. Cancer Res.* **14,** 8205–8212 (2008).
23. Ricci-Vitiani, L. *et al.* Absence of caspase 8 and high expression of PED protect primitive neural cells from cell death. *J. Exp. Med.* **200,** 1257–1266 (2004).

Supplementary Information is linked to the online version of the paper at www.nature.com/nature.

Acknowledgements We thank L. Naldini for providing the lentiviral vectors and S. Forte for gene array data elaboration. This work was supported by grants from Associazione Italiana per la Ricerca sul Cancro.

Author Contributions L.R.-V. and R.P. performed most of the experiments and coordinated the project; M.B. performed cell sorting and flow cytometric analysis; M.T. and G.S. detected and characterized human endothelial cells in mouse xenografts; G.I. and E.A.P. developed the functional assays of the endothelial cell cultures; G.M. recruited the patients and performed surgery; T.C. and L.M.L. were involved in pathology assessment and detection of genomic aberration in endothelial cells; R.D.M. conceived the study and wrote the paper.

Author Information Data have been deposited at the European Bioinformatics Institute (http://www.ebi.ac.uk/arrayexpress/) under accession number E-MEXP-2891. Reprints and permissions information is available at www.nature.com/reprints. The authors declare no competing financial interests. Readers are welcome to comment on the online version of this article at www.nature.com/nature. Correspondence and requests for materials should be addressed to R.D.M. (demaria@iss.it) or R.P. (pallini@rm.unicatt.it).

METHODS

Glioblastoma neurosphere isolation and characterization. Glioblastoma tissue specimens were obtained from adult patients undergoing craniotomy at the Institute of Neurosurgery, Catholic University School of Medicine in Rome. Informed consent was obtained before surgery according to the protocols approved at the Catholic University. Cells were purified through mechanical dissociation of the tumour tissue and cultured at clonal density in a serum-free medium supplemented with EGF and basic FGF as described[3,21,22]. Isolated cells were expanded and characterized both *in vitro* and *in vivo*. In these conditions, cells were able to grow *in vitro* in clusters called neurospheres and maintain an undifferentiated state, as indicated by morphology and expression of stem-cell markers such as CD133, SOX2, musashi and nestin. Such glioma neurosphere cells showed a clonal frequency higher than 10%, ability to coexpress astrocytic as well as neuronal phenotypic markers after serum-induced differentiation *in vitro*, and generation of glial tumours in immunodeficient mice.

Flow cytometry, immunohistochemistry and immunofluorescence. Cell suspension obtained by mechanical dissociation of the tumour tissue from glioblastoma patients from the Institute of Neurosurgery (Supplementary Table 2) was passed through a 100-μm mesh to remove aggregates and stained with fluorochrome-conjugated antibodies to surface antigens. After 1h of incubation on ice, cells were washed twice with PBS and finally resuspended in PBS or in PBS containing 7-aminoactinomycin D (7-AAD) 5μg ml^{-1} to assess viability. Analysis was performed using a fluorescence-activated cell sorter (FACS) Canto flow cytometer (Becton Dickinson). Cell sorting was performed with a FACS Aria cell sorter (Becton Dickinson) equipped with an automatic cloning deposition unit. Cells were selected on the basis of physical parameters and fluorescence and were sorted on sterile tubes or on slides depending on their further utilization.

For immunoistochemistry, immunofluorescence and flow cytometry the following antibodies were used: mouse anti-human CD31 (Novocastra); mouse anti-CD31 (Dako); rat anti-mouse CD31 (BD, Pharmingen); rabbit anti-GFAP (Chemicon or Dako); mouse anti-vWF (Dako); goat anti-human Tie2 (R&D Systems); mouse anti-human VEGFR2 (R&D Systems); rabbit anti-Tie2 (Santa Cruz Biotechnology); mouse anti-human CD144 (R&D Systems); mouse anti-SSEA-1 (R&D Systems); mouse anti-human nuclei antigen (Chemicon); rabbit anti-GFP (Molecular Probes) and anti-eNOS (BD, Pharmingen). Validation of antibody specificity for human and mouse endothelial antigens is shown in Supplementary Fig. 12.

Interphase FISH and FICTION on glioblastoma sections. Single- and dual-probe interphase FISH was performed on histological sections of glioblastoma, on cell nuclei extracted from paraffin-embedded sections of glioblastoma, on cells sorted from glioblastoma samples, and on cultured microvascular endothelial cells of glioblastoma as described[3]. Aneuploidy was definened as loss or gain of one or more chromosome FISH signals. Briefly, locus-specific probes for Cep10, Tel19q and LSI22 were used (Vysis). Standard FISH protocols for pretreatment, hybridization and analyses were followed according to the manufacturer's instructions. Histological 4-μm-thick paraffin sections were dewaxed with xylene and digested with proteinase K 1μg ml^{-1} in 0.002 M Tris buffered saline (TBS) for 20 min at room temperature (20 °C). Samples were then dehydrated in a graded ethanol series and subjected to FISH analysis. After specimen/probe denaturation at 73°C for 5 min, the probes (10 μl per slide) were applied to the slides and subsequently incubated overnight at 42 °C for Cep10 and at 37 °C for 10–16 h for LSI22/Tel19q. Post-hybridization procedure included subsequent washing in 50% formamide/2× SSC (30 min at 46 °C) and 2× SSC 0.1% NP40 (5 min at room temperature). Nuclei were counterstained with 4′,6-diamidino-2-phenylindole (DAPI; Vector Laboratories). The slides were studied with an Axioplan fluorescence microscope (Karl Zeiss) that was equipped with the appropriate filter sets (Vysis). Images were captured using a high-resolution black and white CCD microscope camera AxioCam MRm REV 2 (Karl Zeiss). The resulting images were reconstructed with green (FITC), orange and blue (DAPI) pseudocolour using AxioVision 4 multichannel fluorescence basic workstation (Karl Zeiss) according to the manufacturer's instruction. Glioblastoma sorted cells were fixed in a solution of methanol and acetic acid (3:1) for 10 min and then processed for FISH as described.

Laser capture microdissection of vessels from GSC-derived xenografts. We isolated the vascular structures of tumour xenografts using the Laser Capture Microdissection (LCM) System (PixCell IIe, Arcturus; distributed by Euroclone). LCM was performed on CD31-immunostained (M-20, Santa Cruz Biotechnology) paraffin sections (10-μm thick) of tumour xenografts. For each sample, laser power (50–70 mW) and laser duration (1–1.2 ms) were adjusted. The microdissected tissue was then transferred to an LCM cap and the cells were incubated in 100 ml digestion buffer (0.005% proteinase K in tris(hydroxymethyl)aminomethane (TRIS) 0.05M pH 7). Endothelial cell nuclei were isolated using the NE-PER Nuclear and Cytoplasmic Extraction Reagents (Thermo Scientific) following manufacturer recommendations. Successively, nuclei were washed with PBS and fixed in a solution of methanol/acetic acid (3:1). Eight millilitres of nuclei suspension were placed on a positive charged slide and were dried in a 65 °C oven for 30 min.

FISH on cell nuclei extracted from tumour xenografts. To distinguish human endothelial cells from mice cells, we performed FISH analyses using locus-specific probes for Cep10 (Vysis) and a Cy3-conjugate mouse pan-centromeric chromosome (Cambio). FISH protocols for the Cep10 probe were performed as previously described, whereas for the mouse pan-centromeric probe we followed the manufacturer's instructions. Briefly, after enzymatic digestion with 4mgml^{-1} pepsin in NaCl 0.9% pH 1.5 for 20 min at 37 °C, the nuclei were denatured in 70% formamide in 2× SSC for 2min at 70 °C, and were subsequently immersed in ice-cold 70% ethanol and dehydrated through a series of alcohol washes at 79%, 90% and 100%. The probe was denatured for 10 min at 85°C and immediately chilled on ice. After specimen/probe denaturation, probe was applied to the slide and subsequently incubated overnight at 37 °C. After washing, nuclei were then counterstained with DAPI (Vectashield mounting medium with DAPI; Vector Laboratories).

Isolation and culture of human glioblastoma microvascular endothelial cells. Glioblastoma tissue specimens were stored in medium M199 (Gibco) containing penicillin 100Uml^{-1} at 4 °C for less than 24 h before processing. After several washes with PBS/antibiotics, tissue was finely minced using surgical scissors and then incubated for 2–3 h at 37 °C in Dulbecco's medium (Gibco) containing 0.2% bovine serum albumin (BSA), liberase blendzyme 2–2.5 mg ml^{-1} (Roche Diagnostics). Cellular macroaggregates still present after enzymatic digestion were removed by filtration through a 10-μm pore-size filter (Dako), thus obtaining a monocellular suspension. The filtrate was then washed twice with PBS and centrifuged, the pellet resuspended in 1 ml cold PBS/0.1% BSA pH 7.4. Selection of endothelial cells was performed by using CD31 Miltenyi Microbead Kit (Miltenyi Biotech) according to manufacturer's instructions directly on cell suspensions after enzymatic digestion. Purified cell clusters as well as the negative counterparts were separately resuspended in endothelial basal growth medium (EBM Bullet kit; Biowhittaker Cambrex). Cells were plated onto 25-cm^2 culture dishes, previously coated with 1 μg cm^{-2} collagen type I and 1 μg cm^{-2} fibronectin (Sigma), and maintained at 37 °C in an atmosphere of 5% CO_2. After 10–12 h, plated cells were washed three times with cold PBS to favour detachment of nonendothelial cells. The medium was changed every 3 days. Once at confluence, cells were detached by trypsinization with 0.25% Trypsin/EDTA (Gibco) and reseeded on collagen/fibronectin-coated culture dishes at a split ratio of 1:3.A second magnetic selection was performed on plated endothelial cells after 7–10 cell divisions in order to increase the purity of the cultures.

Endothelial function assays. For *in vitro* three-dimensional tube formation assay, twelve microlitres of tail collagen were dropped onto glass coverslips and allowed to polymerize for 1 h at 37 °C. Cells were then seeded on top of the gels at 50,000 cells per well and allowed to incubate. Then endothelial basal medium was added and cells were cultured for 7 days.To quantify the tube formation, image-analysis techniques were used that measure the length of the tubes and the number of the connections. Data were photographically recorded daily. The average total length and mean total number of junctions for different endothelial cords were further analysed using the two-sided Mann–Whitney U test.For microinjections, a Zeiss microscopy with a manipulator was used. Fluorescein (Monico) was prediluted 1:1,000 into medium and injected into three-dimensional culture with a Hamilton, and observed with a Zeiss Axiovision device camera.

To determine the uptake of acetylated LDLs, cells were incubated with 10 mg ml^{-1} DiI-labelled (1,1′-dioetadeeyl-3,3,3′,3′-tetramethylindocarboeyanine perchlorate) acetylated LDL; Molecular Probes) at 37 °C for 4 h. The slides were analysed using a Nikon Eclipse TE300 inverted microscope equipped with a Zeiss Axiovision device camera.

Gene array. Total RNA was extracted from glioblastoma neurospheres, serum-differentiated glioblastoma neurospheres, glioblastoma neurospheres cultivated under endothelial condition and endothelial cells isolated from glioblastoma patients. Normal human umbilical vascular (HUVEC) or microvascular (HMVEC) endothelial cells were used as controls for endothelial gene expression patterns. RNA was labelled and hybridized to Affymetrix GeneChip1.0ST arrays following the manufacturer's instructions. Hybridization values were normalized by the robust multiarray averaging (RMA) method and hierarchical clustering, with average linkage method, was performed according to samples' gene expression profile. Full data were submitted to ArrayExpress under the accession number E-MEXP-2891.

Lentiviral infection. Selective targeting of the cells expressing endothelial phenotype was obtained by modifying the pRRLsin.Tie2p.TKiresGFP.spre lentiviral vector provided by L. Naldini[15,16]. Viral particle production and GSC infection were performed as previously described[23].

***In vivo* experiments.** Studies involving animals were approved by the Ethical Committee of the Catholic University School of Medicine in Rome. Nude athymic

and SCID mice (female, 4–5 weeks of age; Charles River) were used. For subcutaneous xenografts, cells were resuspended 1×10^6 in 0.1 ml of cold PBS, mixed with an equal volume of cold Matrigel (BD Bioscience), and injected into the flanks of nude mice. For intracranial xenografts, 2×10^5 cells in 5 μl of PBS were injected stereotactically onto the striatum. Mice were killed by 16–20 weeks after grafting to collect tumour xenografts. On ganciclovir treatment, no major toxicity was observed in vital organs.

CORRECTIONS & AMENDMENTS

ERRATUM

doi:10.1038/nature09734

Tumour vascularization via endothelial differentiation of glioblastoma stem-like cells

Lucia Ricci-Vitiani, Roberto Pallini, Mauro Biffoni, Matilde Todaro, Gloria Invernici, Tonia Cenci, Giulio Maira, Eugenio Agostino Parati, Giorgio Stassi, Luigi Maria Larocca & Ruggero De Maria

Nature **468,** 824–828 (2010)

In Fig. 3b of this Letter, the black bar was inadvertently labelled as mCD31 instead of hCD31 (human CD31). The corrected Fig. 3b is shown below.

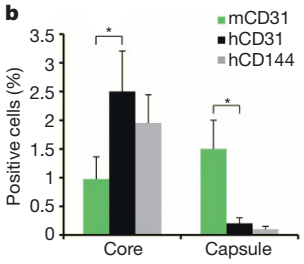

CORRIGENDUM

doi:10.1038/nature10410

Tumour vascularization via endothelial differentiation of glioblastoma stem-like cells

Lucia Ricci-Vitiani, Roberto Pallini, Mauro Biffoni, Matilde Todaro, Gloria Invernici, Tonia Cenci, Giulio Maira, Eugenio Agostino Parati, Giorgio Stassi, Luigi Maria Larocca & Ruggero De Maria

Nature **468,** 824–828 (2010)

The figures and Supplementary figures of this Letter are affected by errors and improper editing. The correct figures are now provided, with an explanation of the variations. The original Letter has not been corrected online. We apologise for the confusion that our errors could have produced. We admit our negligence in the supervision of technical activity. We acknowledge that image manipulation is not acceptable and that any image modification must be clearly described. None of the alterations have any direct impact on the validity of our conclusions, which were also substantially confirmed in papers published by other independent groups[1,2].

In Fig. 1b, the left panel was generated by joining different fields acquired from several pictures in which the density of nuclei was very low. This was not apparent in the original figure because no border limits the individual acquisitions. This does not affect the interpretation of the results, which was based on the direct observation of a large number of cell nuclei by a senior investigator that gave the frequency of euploid versus aneuploid cells in each case preparation. The figure is only intended to show the appearance of different patterns. The same correction has been made in the right panel. Figure 1b, now showing the eight separate images, is corrected below. The master pictures of the figure are available as Supplementary Figs 1 and 2 of this Corrigendum. In Fig. 1c, two parts of the same picture were cut, flipped and moved closer to save space in the figure. However, the upper and lower panels of Fig. 1c partially overlapped. In Fig. 2b, the panel showing the uptake of LDL by HMVEC (bottom image only) erroneously showed a duplication of the GBM patient panel. The HMVEC panel of Fig. 2b is corrected below.

Further errors in the Supplementary Information of the original Letter are described and corrected in the Supplementary Information of this Corrigendum.

Supplementary Information is linked to the online version of the Corrigendum at www.nature.com/nature.

1. Wang, R. *et al.* Glioblastoma stem-like cells give rise to tumour endothelium. *Nature* **468,** 829–833 (2010).
2. Soda, Y. *et al.* Transdifferentiation of glioblastoma cells into vascular endothelial cells. *Proc. Natl Acad. Sci. USA* **108,** 4274–4280 (2011).

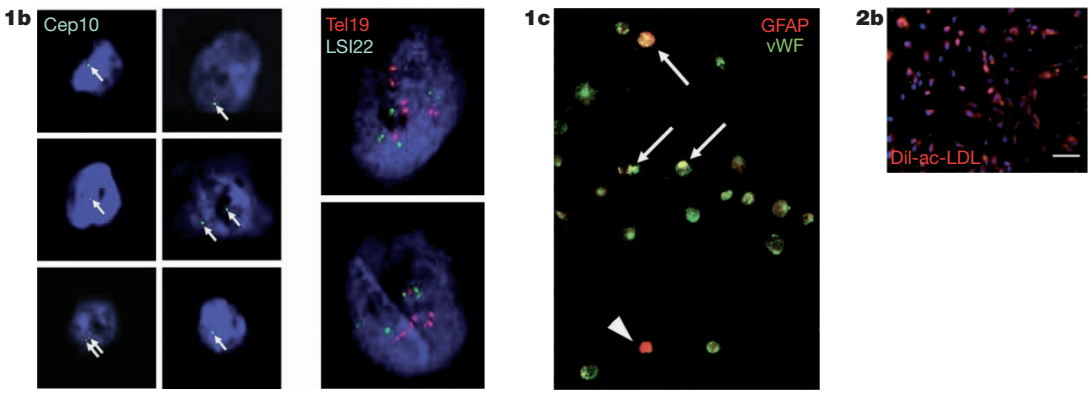

Figure 1 | Corrected left panel of original Fig. 1b, corrected original Fig. 1c, and corrected HMVEC panel in original Fig. 2b.